pISSN 2320-6071 | eISSN 2320-6012

Case Series

DOI: https://dx.doi.org/10.18203/2320-6012.ijrms20253619

Enhanced surgical planning with 3D modeling in pediatric surgical oncology: management of complex abdominal tumors in a low-income country

Ivan Bautista Hernández¹, Daniella Andrea Ponce de León Camargo¹*, Luis Felipe Zarazúa Orozco¹, Andrea Elis Irigoyen², Ma de Lourdes Vega Vega²

Received: 19 August 2025 Revised: 19 September 2025 Accepted: 08 October 2025

*Correspondence:

Dr. Daniella Andrea Ponce de León Camargo, E-mail: daniellaponcedeleon@gmail.com

Copyright: © the author(s), publisher and licensee Medip Academy. This is an open-access article distributed under the terms of the Creative Commons Attribution Non-Commercial License, which permits unrestricted non-commercial use, distribution, and reproduction in any medium, provided the original work is properly cited.

ABSTRACT

Three-dimensional (3D) modeling has emerged as a valuable tool in pediatric oncologic surgery, particularly for complex abdominal tumors where precise anatomical planning is critical. It enables enhanced surgical visualization, improved team communication, and more accurate estimation of vascular structures and adjacent organs, thereby increasing the safety and feasibility of extensive resections. We present six pediatric cases of complex abdominal tumors, including a NOS hepatic tumor, myofibroblastic tumor, cholangiocarcinoma, hepatoblastoma, neuroblastoma, and a Frantz-Gruber tumor, where 3D reconstruction and printing were employed to support preoperative planning and intraoperative navigation. All patients underwent contrast-enhanced thoracoabdominal CT, angiography, and 3D modeling due to tumor size, anatomical complexity, and vascular involvement. Additionally, we performed a literature review to contextualize the clinical value of 3D modeling in pediatric surgical oncology. Six patients underwent complete resections without complications. One patient was deemed unresectable after a detailed 3D evaluation, and only one patient presented a postoperative complication. The models were used to assess tumor boundaries, vascular proximity, and residual liver volume. They also improved interdisciplinary coordination and communication with families. 3D modeling facilitates individualized surgical planning, enabling more accurate, safer, and potentially curative interventions in patients with complex tumors. It enhances communication across the surgical team, supports medical education, and minimizes potential complications. As this technology becomes more accessible, it has the potential to significantly improve outcomes in pediatric surgical oncology.

Keywords: 3D modeling, Pediatric surgery, Abdominal tumors, Surgical planning, Low-income country

INTRODUCTION

The surgical resection of abdominal tumors is a key aspect of treating certain types of pediatric cancer.¹ Cancer in children represents less than 2% of the total malignancies worldwide.¹ Abdominal tumors like neuroblastoma represent 8%, being the 4th most common cause of cancer.¹

While hepatic tumors account for only 1%, being the 9th most common tumor in the pediatric age.¹ The incidence and prevalence of the inflammatory myofibroblastic tumor remain unclear due to the tumor's rare occurrence.²⁻²⁰ Likewise, Frantz tumor is a rare tumor occurring only in 1-2% of all pancreatic tumors. Incidence is almost exclusively seen in young females in 91% of cases.¹⁷, ²¹⁻²⁵

¹Department of Pediatric Surgical Oncology, Anillo Vial Fray Junipero Serra N 1999 Col. Rancho Menchaca, Querétaro, Mexico

²Department of Clinical Pediatric Oncology, Anillo Vial Fray Junipero Serra N 1999 Col. Rancho Menchaca, Querétaro, Mexico

The neuroblastoma diagnostic approach begins by defining image risk factors by performing a contrast-enhanced CT scan to classify the tumor according to the INRG staging system and detection of catecholamines in urine; histopathologic study confirms it after performing a bone marrow biopsy, which determines the NMYC amplification (±) and the mitosis-karyorrhexis index to assign the risk stratification.^{1,4}

Hepatic tumor diagnosis begins with measuring alphafetoprotein (AFP) and human chorionic gonadotropin (hCG), and a contrast-enhanced CT or MRI to classify the tumor according to the pretext classification. The surgery must be done at diagnosis if images show the tumor as a pretext I or II. In tumors classified as pretext II with less than 1 cm of healthy hepatic tissue between the tumor and the mid-hepatic vein, and in tumors classified as pretext III and IV, the biopsy is mandatory to start neoadjuvant chemotherapy. According to the histopathological results, the subsequent management will be determined either by neoadjuvant chemotherapy or primary resection, if feasible, based on imaging studies.

In the case of a diagnosis of cholangiocarcinoma, staging will be carried out according to the American joint committee on cancer (AJCC) to define whether it is possible to perform the surgery or not.³

The children's hepatic tumor international collaboration (CHIC) recommends early communication with a center that has the resources to perform a liver transplant and discourages super hepatectomies for all posttext tumors with intrinsic vascular involvement and all posttext IV multifocal tumors.²

The treatment of hepatic tumors and neuroblastoma varies mainly in the use of neoadjuvant chemotherapy; in the case of neuroblastoma, the primary tumor undergoes four cycles of chemotherapy, subsequently the surgical resection is performed, and as last line of treatment, the autologous stem rescue is reserved.⁴

Solid pseudopapillary neoplasm of pancreas, also known as the Frantz-Gruber tumor, is an uncommon pancreatic tumor. ^{15,17-19} This entity is characterized by a low malignant potential and is most often located in the body and tail of the pancreas. Nevertheless, in pediatric populations, the most frequent site of origin is pancreatic head, and it commonly affects females. ¹⁵ Clinically, presentation is nonspecific. Once the disease progresses, it begins to cause early satiety, nausea, and vomiting secondary to a mass effect. ¹⁸ Radical resection remains the treatment of choice for malignant pancreatic tumors;

however, a parenchyma-sparing procedure should be performed to reduce complications and preserve pancreatic function.¹⁹

myofibroblastic The inflammatory tumor is mesenchymal neoplasm defined by the proliferation of spindle-shaped myofibroblasts accompanied by a dense inflammatory infiltrate.^{21,22} It is typically classified as a benign tumor; it exhibits intermediate malignant potential, with a tendency for local recurrence in cases of incomplete resection.²⁴ While its most common presentation is in the lungs, it can appear in any anatomical region, soft tissues. and abdominal organs in pediatric patients.^{22,23} In the specific case of the hepatic presentation, symptoms may include abdominal pain, fever, biliary obstruction, or signs of portal hypertension caused by obliterative phlebitis. 21,23 The definitive diagnosis is by histopathological evaluation and immunohistochemical analysis, with approximately 50% of cases demonstrating ALK gene rearrangements and ALK protein overexpression.²² Complete surgical resection remains the primary therapeutic approach, aiming to achieve local control of the disease.²⁴

3D modeling has been around since 1987, but it has recently gained the attention of surgeons, as evidenced by the increasing number of case reports published in recent years. ¹⁴ The 3D modeling utilizes different materials and colors to represent various anatomical features and their relationships with the tumor in an accurate and personalized manner. ^{5,11,12} These models take the contrastenhanced CT scans of each patient and create a 3D image that can be manipulated to help the surgical team better understand, measure, and practice the dissections.

CASE SERIES

We utilized the digital imaging reconstruction 3D software. In all six cases, we requested virtual modeling, and in cases 2-6, we also requested a 3D printed model. The inclusion criteria to be considered a candidate for 3D modeling were as follows: Patients with neuroblastoma classified as L2, Hepatic tumors classified as pretext III and IV, mechanical compression of the biliary tract and/or adjacent structures, Intimate involvement of vascular structures and Invasion of adjacent structures. We present six patients who arrived within the last two years, summarized in Table 1. All patients underwent a contrastenhanced thoraco-abdominopelvic CT scan using a 16slice CT scanner and an abdominal angiography MRI using a 1.5 Tesla MRI scanner. These imaging studies were performed to assess tumor's extent, determine whether adjacent structures were invaded, and evaluate the presence and degree of vascular involvement.

Table 1: Summary of pediatric patients with complex abdominal tumors in which 3D modeling.

Cases	Age (in years)/ sex	Diagnostic	Classification	Type of Surgery	3D model use	Outcome
1	10/ M	Hepatic tumor (NOS)	Pretext IV	Extended right hepatectomy	Virtual	Complete resection without complications

Continued.

Cases	Age (in years)/ sex	Diagnostic	Classification	Type of Surgery	3D model use	Outcome
2	4/ M	Myofibroblastic hepatic tumor	Pretext III D	Non-resectable	Virtual + printed	Irresectable; chemotherapy initiated
3	14/ F	Cholangiocarcinoma	Pretext IV	Extended right hepatectomy	Virtual + printed	Complete resection.
4	2/ F	Neuroblastoma	INRGSS L2	Retroperitoneal lymphadenectomy + right nephrectomy	Virtual + printed	Complete resection without complications
5	3/ F	Hepatoblastoma	Pretext IV → posttext II	Left hepatectomy	Virtual + printed	Complete resection; no complications
6	10/ F	Frantz-Gruber tumor	No classification	Whipple procedure	Virtual + printed	Complete resection without complications

Case 1

A 10-year-old male patient with no relevant medical history arrived with headache and nausea, accompanied by pre-prandial vomiting, generalized pain, and abdominal distension. On physical examination, he had xanthomas and a distended abdomen due to hepatomegaly not extending past the midline.

The contrast-enhanced thoraco-abdominopelvic CT scan revealed a solid, heterogeneous hepatic mass with calcifications involving the right and middle hepatic veins, the right hepatic artery, and the right portal vein, resulting in compression of the cava. A biopsy was carried out via laparoscopy, and the histopathological study revealed a not otherwise specified hepatocellular neoplasm. Afterwards, an abdominal angiography MRI (Figure 1 A) was performed, revealing a space-occupying lesion affecting segments V, VI, and VIII, with well-defined borders that caused lobulation of the hepatic edge. This mass had dimensions of $15.5 \times 10.5 \times 11.7$ cm. The tumor was classified as a pretext IV, and a 3D model was requested (Figure 1 C and D).

3D model showed tumor extending approximately 1.3 cm into segment II, making this tumor pretext IV. An extended right hepatectomy was carried out, successfully resecting tumor entirely with no complications (Figure 1 B).

Intraoperative navigation

The Three-dimensional model identified a 1.5 cm vascular structure draining from the right hepatic lobe to the vena cava, which no other imaging studies had shown. During the procedure, we found an accessory branch of the right portal vein. Using the virtual model, we confirm the location of the portal bifurcation, allowing us to clamp and dissect the right portal vein and its accessory vein, without damaging the left portal vein. Before the hepatic dissection, the three-dimensional model was used to locate and loop the three hepatic veins upon arriving at the vena cava. From the exit of the left hepatic vein and following the tumor perimeter in the 3D model, we began dissecting the liver, avoiding a 1.3 cm transgression of the tumor into

the segment II, and preserving the venous drainage. The anatomical precision of the 3D model allows a clean hepatic transection with a harmonic scalpel handpiece, leaving a 0.5 cm margin.

Case 2

A 4-year-old male patient with no relevant medical history began his current condition six months before his arrival with melena, hematemesis, jaundice, weight loss, dark urine, and diffuse abdominal pain. On physical examination, the patient presents generalized jaundice, right cervical lymphadenopathy, a double percutaneous drainage on the abdomen, and hepatomegaly. A liver biopsy was carried out at an external hospital at the time when the percutaneous drainages were placed, which reported a hepatic mesenchymal hamartoma and an ulcerated hamartomatous polyp in the stomach.

A contrast-enhanced thoraco-abdominopelvic CT scan was performed, revealing hepatomegaly heterogeneous hepatic lesion in segment IV with central calcification, which compressed the extrahepatic bile duct caused intrahepatic dilation. Additionally, multilobular thickening was noted on the anterior wall of the gastric fundus and body, with areas of central necrosis. An abdominal angiography MRI, along with a magnetic resonance cholangiopancreatography (Figure 2 A), was also performed, which revealed a lesion in the anterior wall of the gastric fundus and a hepatic tumoral lesion in segment IVb, causing intrahepatic bile duct dilation. The tumor was classified as a pretext III D, and a 3D model and impression were requested (Figure 2 B).

The model showed that tumor compressed the confluence of the right and left hepatic ducts along with the common hepatic duct. After virtually removing segments IVa and IVb and isolating the intrahepatic bile duct, the model showed that the tumor reached far beyond into the hepatic parenchyma granting the resection impossible due to the lack of common right and left ducts to perform a biliodigestive derivation (Figure 2 C). Based upon the 3D model, we decided surgical resection was impossible, and that the best approach was to perform another liver and

gastric biopsy which revealed the final diagnosis that was a myofibroblastic tumor. During procedure, a bile duct exploration was conducted, during which the contrast did not pass through common hepatic duct.

Case 3

A 14-year-old female patient with no significant medical history began her condition with an 8-month history of amenorrhea and weight loss. An abdominal ultrasound reported a mass, and she was subsequently referred to our hospital. On physical examination, the abdomen was distended due to hepatomegaly, with liver edge palpable near the iliac crest and not crossing the midline. There was tenderness on palpation in the epigastric region and right iliac fossa, with an abdominal perimeter of 77 cm.

A contrast-enhanced thoraco-abdominopelvic CT scan and abdominal MRI angiography performed (Figure 3 A), revealing an enlarged liver with a solid-appearing heterogeneous hepatic infiltrative lesion. Its approximate dimensions were 10.9×13.7×17 cm, involving segments IVa, Vb, V, VI and VIII. Lesion surrounded middle hepatic vein, causing collapse of gallbladder and extrinsically displacing inferior vena cava and aorta contralaterally. It also displaces ipsilateral kidney caudally.

The tumor was classified as a pretext IV. A liver biopsy was carried out via laparoscopy, and the histopathological study reported moderately differentiated adenocarcinoma consistent with cholangiocarcinoma. A 3D model (Figure 3 C) and impression (Figure 3 D) were requested, and an extended right hepatectomy was carried out (Figure 3 B).

Intraoperative navigation

The virtual model was used to define the dimensions of the liver and the tumor, and to simulate the remaining parenchyma after the surgery to determine if the ressection was possible. The software showed an initial hepatic parenchyma to be 2994.56 ml, of which the tumor represented 2305.81 ml. After the virtual removal of the tumor, the model reported a remaining parenchyma of 688.74ml, representing 23% of remaining hepatic tissue, making it possible to go ahead with the resection.

During the dissection of the hepatic hilum, the difference between the cystic duct and the hepatic artery was unclear. The 3D model showed a redundant cystic conduct, approaching laterally to the common bile duct, and the hepatic artery being cephalic immediately beneath the hepatic parenchyma. This allowed a safe dissection of the cystic conduct without further manipulation of the common bile duct and absolute certainty of preserving the hepatic artery.

Case 4

A 2-year-old female patient with no significant medical history began two months before her arrival with weight

loss and abdominal pain associated with constipation. Upon her arrival, a physical examination revealed left cervical lymphadenopathy, a distended abdomen due to a right abdominal mass with an irregular consistency that does not extend past the midline, pain on palpation, and decreased peristalsis. The tumor was classified as an L2 according to the INRGSS. A bone marrow biopsy and an abdominal biopsy via laparoscopy were performed. The histopathological study reported a poorly differentiated neuroblastoma with low schwannian stroma, low mitotic activity, and a low karyorrhexis index, without necrosis or vascular permeation. The molecular analysis revealed NMYC amplification. A contrast-enhanced thoracoabdominopelvic CT scan (Figure 4 A) was performed, showing right kidney with loss of its typical morphology. The scan identified a lobulated lesion with well-defined borders. heterogeneous in composition with a predominantly solid component, and coarse calcifications surrounding the renal vein, artery, inferior vena cava, and abdominal aorta. Its approximate dimensions were 6×7.8×8.1 cm. Paraaortic and left iliac chain lymph node conglomerates were identified, with the largest measuring 2.1×1.9 cm. An abdominal MRI angiography was carried out, revealing that right kidney had lost its usual morphology due to a lobulated lesion with well-defined borders and predominantly solid component. Approximate dimensions were 6.1×8×7 cm. Paraaortic lymph node conglomerates were identified, with the largest measuring 2.7×2 cm. A virtual 3D model and impression were requested (Figure 4 C), before the surgery, 4 cycles of chemotherapy following COG protocol were administered as neoadjuvant chemotherapy, and later on, retroperitoneal lymphadenectomy was carried out.

Intraoperative navigation

This was a large and anatomically complex tumor involving several structures; the three-dimensional model was particularly useful in locating the tumor in its proximity to vascular structures. During the procedure, the fiscal model was used to determine the extent to which we could dissect (Figure 4 B) without encountering vascular structures, particularly during the resection of the right paracaval component along with the inter-cavo-aortic extension and the right iliac component, while the virtual model was key to proceeding with the right nephrectomy along with the adrenal gland and the lymphatic components.

By virtually dimming the tumor, the team was able to observe how the tumor extended into the right renal hilum, covering the cava, intercavo-aortic plane, paraaortic, and into the left renal hilum. Showing how the dissection could be carried out, protecting the celiac artery and superior mesenteric artery.

Case 5

A 3-year-old female patient with a history of prematurity at 32 weeks of gestation, early-onset neonatal sepsis,

patent foramen ovale, and fatty liver began three weeks before her arrival with diarrhea and increased abdominal circumference. On her arrival, the physical examination revealed a distended abdomen due to an epigastric tumor with irregular borders; the liver was palpable 5 cm below the costal margin. A contrast-enhanced thoracoabdominopelvic CT scan was carried out, revealing an enlarged liver due to a parenchymal lesion with partially lobulated borders defined, and heterogeneous enhancement in both the arterial and venous phases (Figure 5 A) The lesion involves all hepatic segments, partially sparing segment VI, crosses midline, compresses the inferior vena cava, and displaces adjacent organs. It measures 14×13.5×10 cm. The tumor was classified as a pretext IV, and four cycles of neoadjuvant chemotherapy were administered following the PHITT protocol. After 11 weeks of treatment, an abdominal MRI angiography was performed, which revealed an oval-shaped lesion with lobulated borders and a capsule, measuring approximately 6.7×4.3×6.5 cm, with a volume of 97 ml. It involves segments IVA, IVB, VI, and VII, and the tumor was classified as a postext III (Figure 5 B). A virtual 3D model and impression were requested, and a left hepatectomy was carried out with no complications (Figure 5 C).

Intraoperative navigation

The three-dimensional model revealed numerous non-identified vessels from the retrohepatic cava to segment V, as well as the tumor and the common bile ducts; the conventional imaging exams performed in our hospital did not show any of these findings. This demonstrated neovascularisation and early signs of portal hypertension, allowing the team virtual guidance in the retrohepatic space, leading to vascular control and dissection without manipulation or damage to the right portal vein. To dissect the hepatic parenchyma, the 3D model was used to locate the confluence of the hepatic veins, before entering the

vena cava, as the model showed the middle hepatic vein precisely dividing the tumor into the parenchyma. The middle hepatic vein lateral border was used to guide the sonic dissector through the healthy liver, resulting in a 34.97% remaining parenchyma.

Case 6

A 10-year-old female presented with an 8-day history of abdominal pain. vomiting. and fever. Physical examination revealed jaundice, with otherwise normal findings. Laboratory results showed an elevated direct bilirubin (10 mg/dL), suggestive of cholangitis. Abdominal ultrasound shows a hyperechogenic lesion in the pancreatic head. To confirm the diagnosis, a contrastenhanced CT was ordered, which revealed a mass causing biliary tract dilatation. Lastly, an MRI confirmed the presence of a tumor in the head of the pancreas (Figure 6 A) A virtual 3D reconstruction and a physical 3D-printed model of the tumor and surrounding anatomy were utilized to perform a pylorus-preserving pancreato-duodenectomy (Whipple).

Surgical advantages observed in the OR.

Intraoperative navigation

During surgery, we realised that the tumor was completely attached to the common portal vein, as well as to the superior mesenteric vein. The 3D model (Figure 6 D) was helpful in this particular case by showing us how attached the tumor was to the duodenum, the dilation of the common hepatic duct, and multiple affluents arising from the portal vein. This allowed an appropriate approach, avoiding dissecting the duodenum immediately anterior to the tumor, rather dividing the tumor from the porta and superior mesenteric vein, freeing the tumor before its dissection along with the duodenum (Figure 6 B).

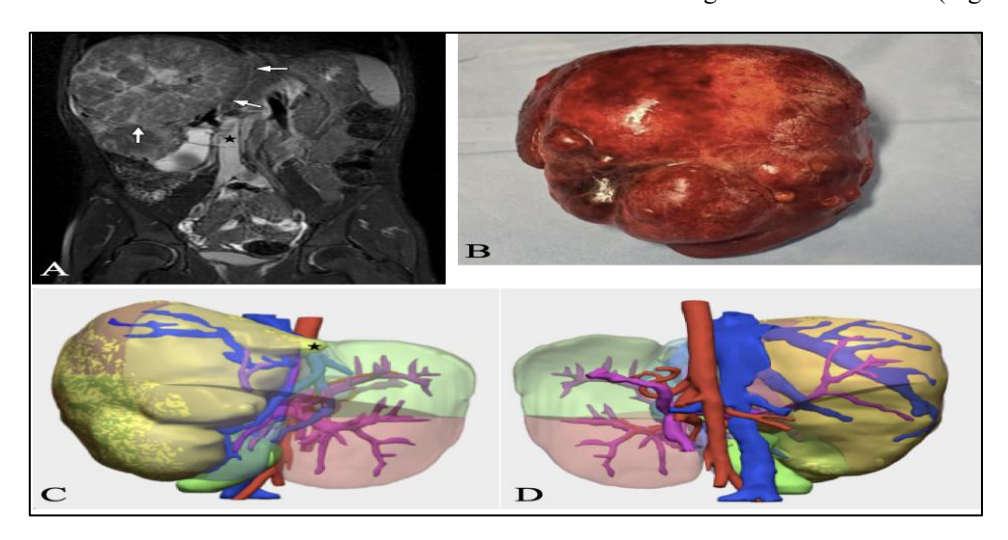


Figure 1 (A-D): A) Abdominal angiography MRI showing a large intrahepatic mass (arrows) compressing the inferior vena cava (star). B) Surgical specimen of segments IV-VIII with tumor-related destruction. C-D) Virtual 3D liver model with semi-translucent segments, displaying the tumor in yellow (star) and intrahepatic vascular anatomy (arteries in pink, veins in blue).

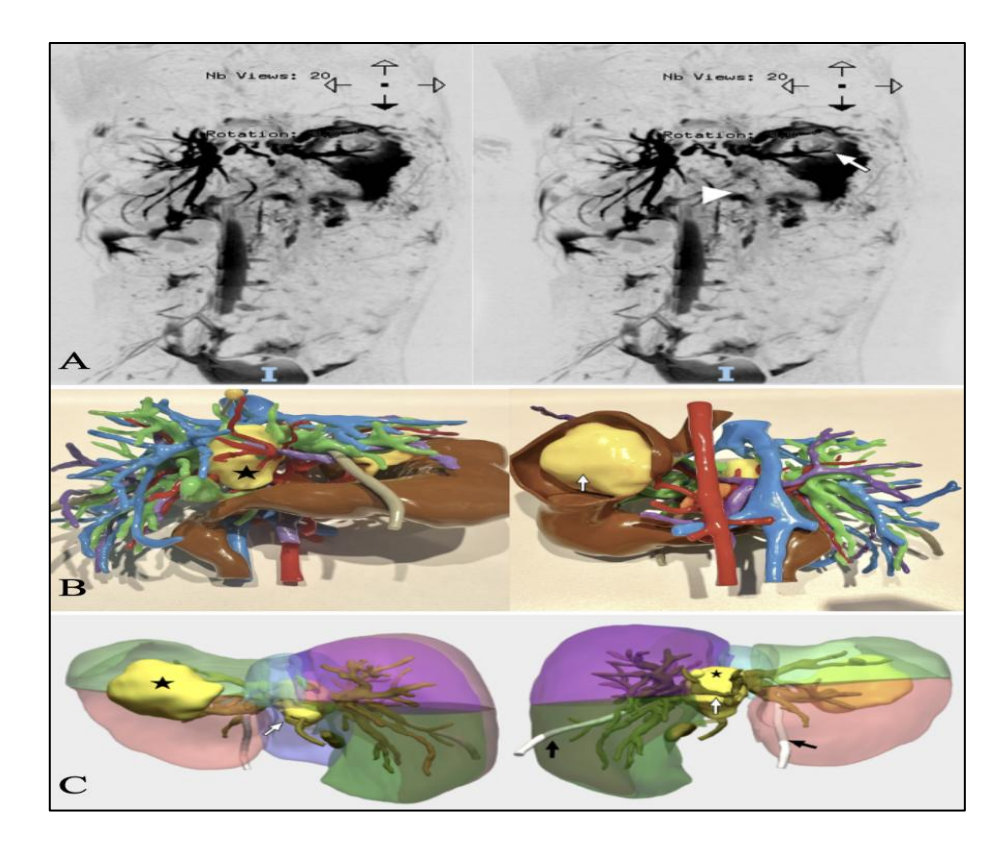


Figure 2 (A-C): A) Magnetic resonance cholangiopancreatography showing a fundus wall defect (arrow) and obstruction of the common hepatic duct (triangle). B) Printed 3D model: anterior and posterior views highlighting vascular/biliary structures and the tumor in yellow (star). C) Virtual 3D model: posterior and anterior views with translucent hepatic segments showing the gastric tumor (star), its relation to the common bile duct (arrow), and external biliary catheters (black arrows).

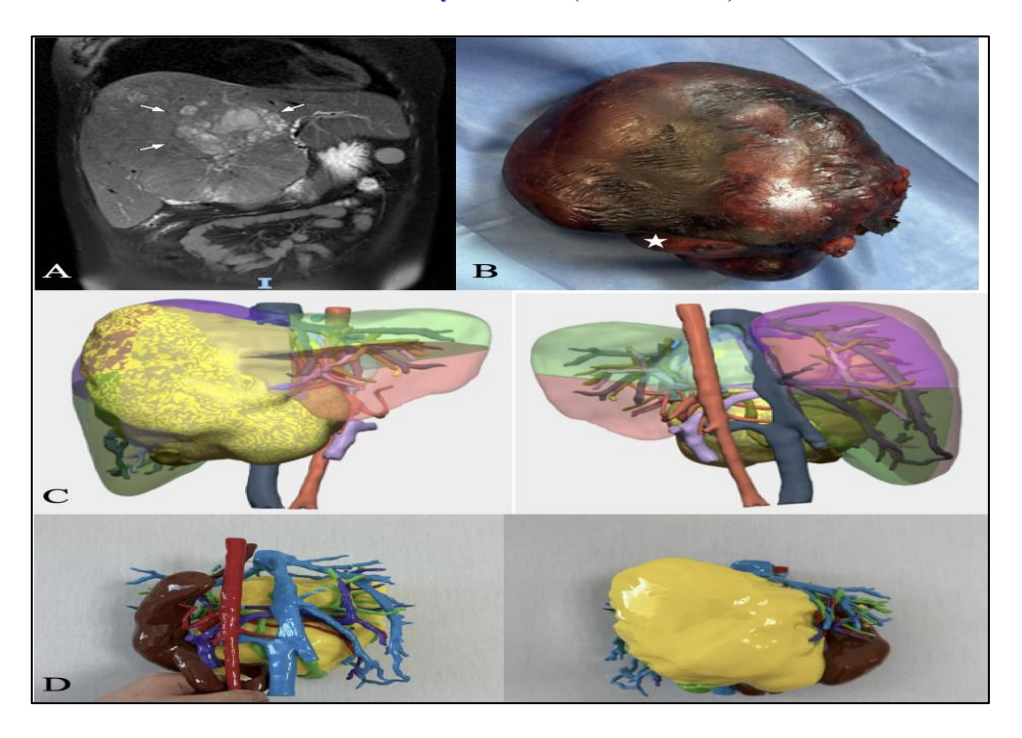


Figure 3 (A-D): A) Abdominal angiography MRI, showing a central lesion measuring 172×139×1108 mm in the right and caudate lobe (Arrows). B) Surgical piece, containing gallbladder (Star) and segments IVa, IVb, V, VI, VII, and VIII. Clearly showing signs of deformation and anatomical destruction of the liver parenchyma. C) Virtual 3D model. Hepatic tumor in yellow, sparing segments II and III. D) 3D model impression, showcasing the tumor in yellow and its relation to the stomach in brown.

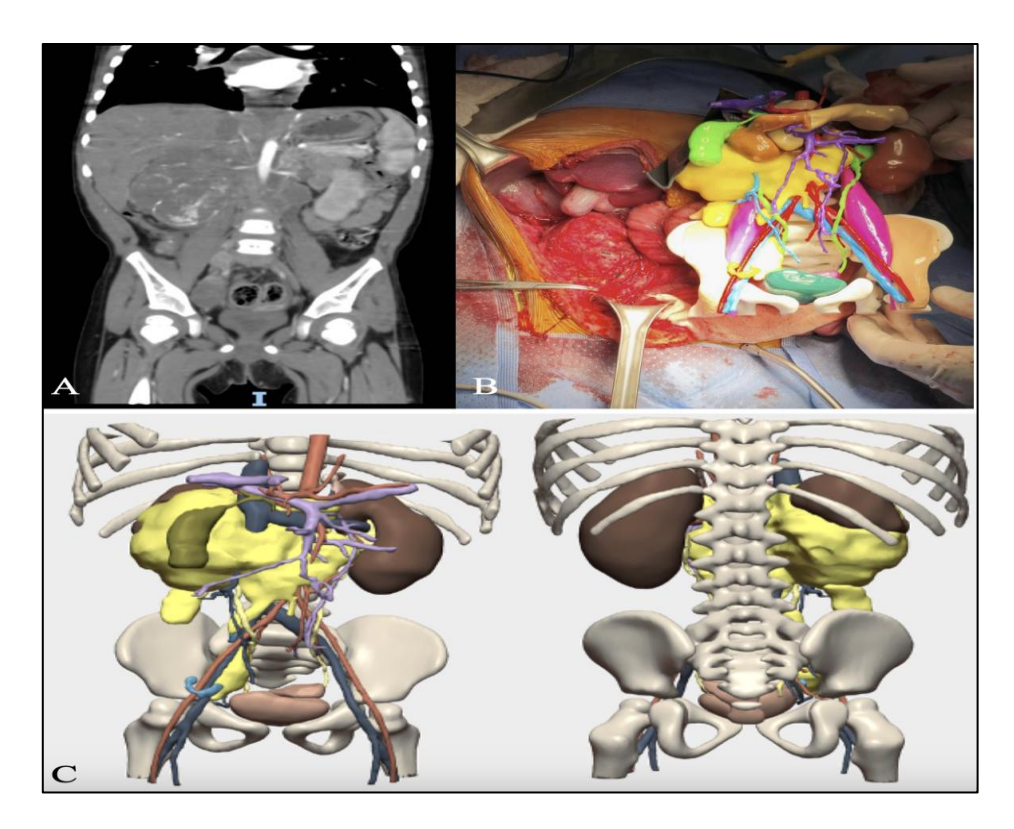


Figure 4 (A-C): A) Contrast-enhanced thoraco-abdominopelvic CT scan. B) Retroperitoneal lymphadenectomy using the printed 3D model. C) Virtual 3D model.

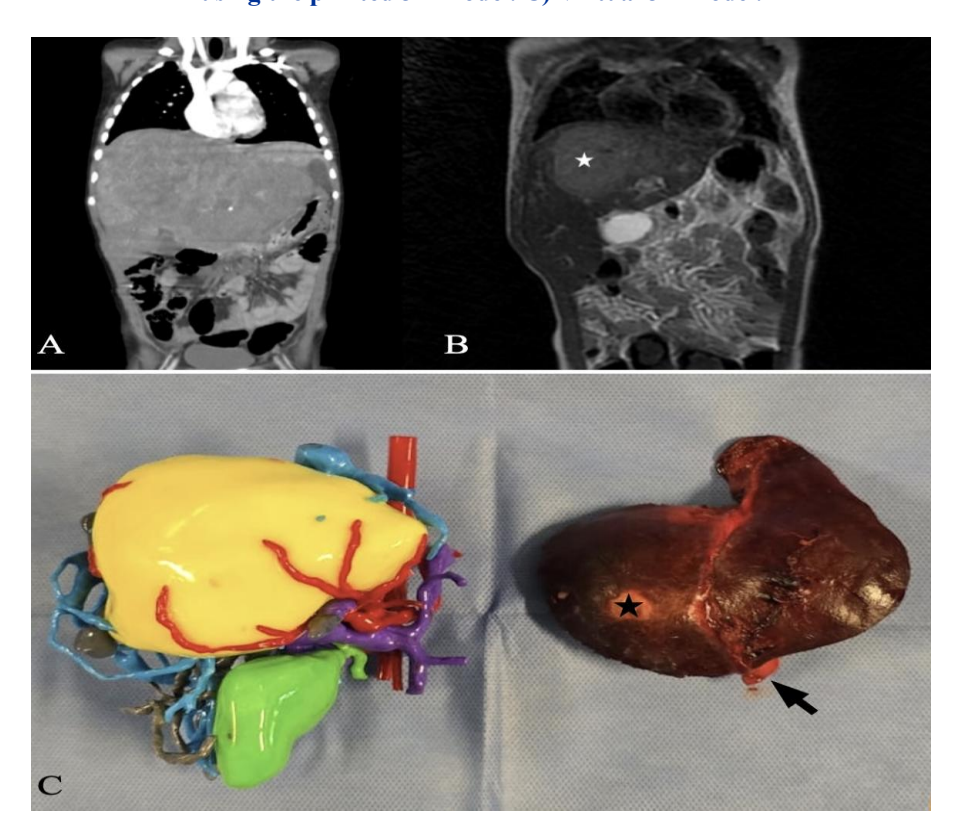


Figure 5 (A-C): A) Pre-treatment CT scan showing hepatomegaly with a 14×13.5×10 cm tumor compressing adjacent organs and the inferior vena cava. B) Post-treatment CT scan demonstrating tumor reduction to 6.7×4.3×6.5 cm (star) and normalization of liver size. C) Printed 3D model and surgical specimen: tumor in yellow adjacent to the left hepatic duct and vessels; specimen shows central mass (star) and duodenal ligament enlargement indicating portal hypertension (arrow).

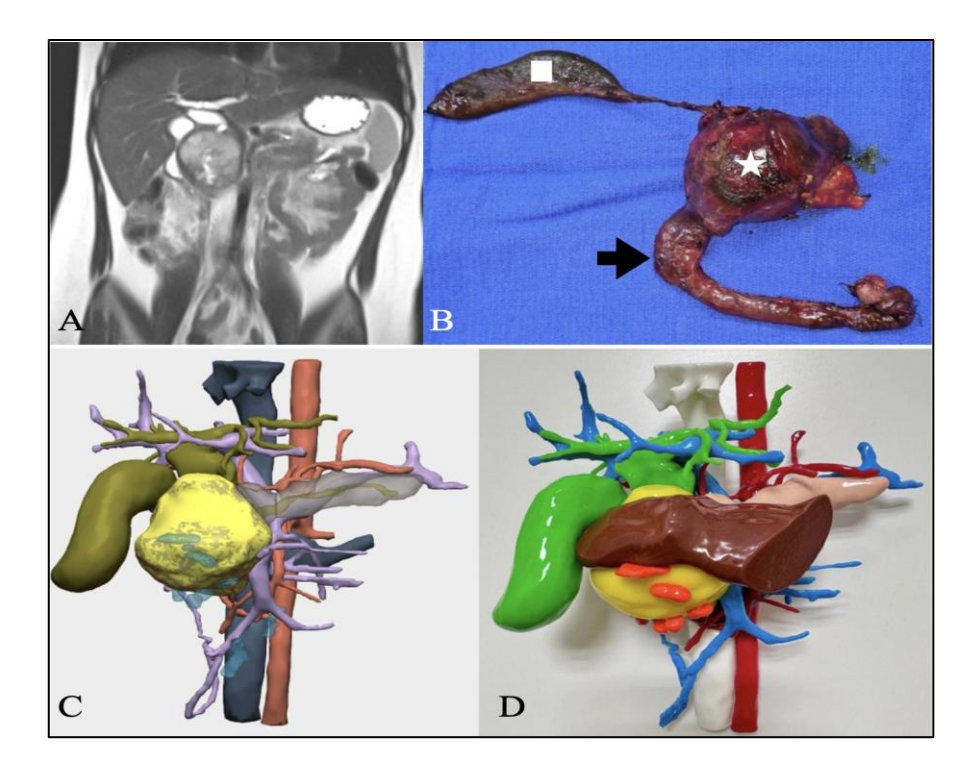


Figure 6 (A-D): A) Tumor in the pancreatic head causing biliary tract dilatation. B) Surgical specimen showing the tumor (star), duodenum (arrow), and gallbladder (square). C) Virtual 3D reconstruction showing the tumor (yellow), portal vein (green), intrahepatic bile duct, and gallbladder. D) 3D-printed model with stomach segment (yellow) and involved ganglion (orange).

DISCUSSION

In countries like ours, late diagnoses constitute a significant challenge primarily due to limited access to social security and healthcare services. This situation often results in patients presenting with advanced-stage disease, which leads many secondary-level centers to offer palliative care as the only therapeutic option. Furthermore, these centers frequently face resource and budget constraints that limit the adequate management of such tumors.

In this context, where not all therapies are available due to a lack of resources or adequate logistics within the country, three-dimensional reconstruction and printing have become strategic resources, translating conventional CT and angiography data into tangible, patient-specific models. We can simulate resections and delineate vascular anatomy before entering the operating room. This technological bridge helps by providing other therapeutic approaches to offer our patients a surgical option, enabling "greater and safer resections, thereby improving the surgical management of complex tumors".⁵

These platforms provide a patient-specific and tangible representation of the tumor and its surrounding anatomical environment. 3D reconstructions deliver greater spatial awareness and anatomical detail than two-dimensional imaging modalities, allowing surgeons to plan resections, anticipate vascular challenges, and mitigate intraoperative risks more effectively. 8 As a result, these technologies help

reduce the incidence of complications associated with distorted anatomy due to tumor extension.

In high-income countries, extended hepatic resections are rarely performed due to their strong association with complications such as liver insufficiency, impaired hepatic performance, cholestasis, massive hemorrhage, and fluid overload. These adverse outcomes arise from the excision of significant portions of the liver, compromising the functionality of the remaining parenchyma. The mortality associated with extended hepatectomy approximately 5%, while the morbidity rate reaches up to 50%.6 This elevated risk profile is a primary reason why this procedure has been widely abandoned. The emergence of perioperative and postoperative complications has been directly linked to the number of hepatic segments removed. Recurrence rates among patients undergoing liver resections were higher than in those who received liver transplants.7

In Mexico, this technique remains one of the few viable therapeutic alternatives, primarily due to the scarcity of resources, limited infrastructure, and the shortage of donor organs for liver transplantation. In a country with over 126 million inhabitants, fewer than 300 liver transplants are performed annually. Within this context, pediatric oncology patients who are ineligible for transplant, as defined by pretext classification, are frequently considered for extended hepatectomy to achieve gross total resection and a disease-free outcome, thereby improving long-term survival.

Beyond their clinical application, 3D printed models serve as outstanding educational tools, especially for surgical trainees and medical students. Liver models fabricated through 3D printing significantly enhance the understanding of hepatic segmental anatomy and its relationship with critical vascular structures such as the portal vein and inferior vena cava. Traditionally, cadaveric dissection was the preferred method for anatomical education, offering spatial orientation and tactile learning. However, the decline in cadaver availability and the logistical burdens of preservation have prompted a shift toward more sustainable alternatives. 3D modeling enables academic institutions to accurately recreate complex anatomy, thereby reducing costs and improving learning efficiency in medical education. If

Despite the promising outcomes observed in our series, this study has certain limitations that should be acknowledged. Although the results support the clinical utility of 3D modeling in complex pediatric abdominal tumors, larger studies across multiple centers would be needed to validate these benefits. The hospital where we conducted this case series is a highly specialized pediatric oncology center equipped with resources that many centers in Mexico do not have access to, making 3D implementation challenging in public modeling institutions. Barriers include limited access to advanced imaging technologies such as contrast-enhanced CT and MRI, the high costs associated with 3D reconstruction services, and the need for institutional infrastructure to support this technology. These constraints make replication of our protocol difficult in many parts of the country, emphasizing the need for broader investment in surgical innovation and imaging accessibility within the national healthcare system.

CONCLUSION

The 3D modeling of abdominal tumors enables us to plan complex resections with meticulous precision, as it is tailored for each patient. Each model emphasizes the intricate anatomy of the tumor and relevant anatomical landmarks, facilitating the anticipation of complications and the optimization of the surgical strategy. This technology expands therapeutic possibilities in countries like Mexico. It has transformed the surgical management of complex abdominal tumors, either by enabling curative resections or by making feasible procedures that would otherwise pose excessive risk.

An additional and highly valuable application of 3D modeling is its ability to calculate future liver remnant (FLR) volume in cubic centimeters. This quantitative feature enables surgeons to accurately estimate the amount of viable hepatic tissue remaining after resection. Particularly in extensive liver surgeries involving pretext III and IV tumors, precise volumetric assessment is essential to reduce the likelihood of postoperative liver failure.

Moreover, 3D modeling has become a valuable educational resource, promoting a deeper understanding of tumor complexity and enhancing the communication of treatment plans to both healthcare professionals and patient families during preoperative consultations. The printed models can be sterilized and used intraoperatively, offering real-time spatial guidance and improving anatomical orientation and surgical precision. When the perioperative team visualizes the tumor and its relationships with surrounding structures, they gain a shared understanding of the technical demands of the procedure.

Although we have highlighted the significant advantages of 3D modeling and its growing adoption across Mexican hospitals, driven by ongoing technological advancements and declining costs, it is important to acknowledge that this work was conducted in a privately funded institution. Unlike our center, many public hospitals in Mexico may lack the necessary infrastructure or budget to incorporate this technology.

If this technology were to become widely accessible in public hospitals across Mexico, it could improve postoperative survival rates and reduce surgical complications. By enabling precise preoperative planning, 3D modeling would help standardize complex procedures and allow surgeons to anticipate anatomical challenges more effectively.

ACKNOWLEDGMENTS

Authors would like to thank to medical and nursing staff of Hospital Infantil Teletón de Oncología (HITO) and to Cella Medical Solutions, who provided the virtual and printed 3D models. And special gratitude to Dr. Javier Leal Ojeda and Dr. Juan Alcantar Fierros.

Funding: No funding sources Conflict of interest: None declared Ethical approval: Not required

REFERENCES

- Losty PD, La Quaglia M, Sarnacki S, Fuchs J, Taguchi T, editors. Pediatric surgical oncology. 1st ed. Boca Raton: CRC Press; 2022.
- 2. Meyers R, Hiyama E, Czauderna P, Tiao GM. Liver tumors in pediatric patients. Surg Oncol Clin N Am. 2020;29(1):1-15.
- 3. Lee AJ, Chun YS. Intrahepatic cholangiocarcinoma: The AJCC/UICC 8th edition updates. Chin Clin Oncol. 2018;7(5):52.
- 4. Chung C, Boterberg T, Lucas J, Panoff J, Valteau-Couanet D, Hero B, et al. Neuroblastoma. Pediatr Blood Cancer. 2021;68(2):e28473.
- Krauel L, Fenollosa F, Riaza L, Pérez M, Tarrado X, Morales A, et al. Use of 3D prototypes for complex surgical oncologic cases. World J Surg. 2016;40(4):1069-75.

- 6. Vauthey JN, Pawlik TM, Abdalla EK, Arens JF, Nemr RA, Wei SH, et al. Is extended hepatectomy for hepatobiliary malignancy justified? Ann Surg. 2004;239(5):722-32.
- Uchida H, Sakamoto S, Sasaki K, Takeda M, Hirata Y, Fukuda A, et al. Surgical treatment strategy for advanced hepatoblastoma: Resection versus transplantation. Pediatr Blood Cancer. 2018;65(8):e27383.
- 8. Youn JK, Park SJ, Choi YH. Application of 3D printing technology for pre-operative evaluation, education, and informed consent in pediatric retroperitoneal tumors. Sci Rep. 2023;13:1671.
- Abdalla EK, Barnett CC, Doherty D, Curley SA, Vauthey JN. Hepatic resection for colorectal liver metastasis: Prognostic factors and long-term survival. JAMA Surg. 2002;137(6):675-81.
- Bautista Sánchez JA, Acosta-Altamirano G, De Santos González LR, Vázquez González KI, Castro-Fuentes CA. A general view of liver transplantation in Mexico. Rev Gastroenterol Mex. 2024;89(4):449-61.
- 11. Zhu J, Wang Z, Zhang X, Zhang Y. Impact of 3D printing technology on comprehension of surgical anatomy of retroperitoneal tumor. World J Surg. 2018;42(6):1710-5.
- 12. Malik HH, Darwood AR, Shaunak S, Kulatilake P, El-Hilly AA, Mulki O, et al. Three-dimensional printing in surgery: A review of current surgical applications. J Surg Res. 2015;199(2):512-22.
- 13. Kong X, Nie L, Zhang H, Wang Z, Ye Q, Tang L, et al. Do 3D printing models improve anatomical teaching about hepatic segments to medical students? A randomized controlled study. World J Surg. 2016;40(8):1969-76.
- Narang P, Raju B, Jumah F, Konar SK, Nagaraj A, Gupta G, et al. The evolution of 3D anatomical models: A brief historical overview. World Neurosurg. 2021;155:135-43.
- 15. Spătaru RI, Enculescu A, Popoiu MC. Gruber-Frantz tumor: a very rare pathological condition in children. Rom J Morphol Embryol. 2014;55(4):1497-501.
- Antoniou EA, Damaskos C, Garmpis N, Garmpi A, Sakellariou S, Dimitroulis D, et al. Solid pseudopapillary tumor of the pancreas: A single-

- center experience and review of the literature. In Vivo. 2017;31(4):501-10.
- 17. Jáquez-Quintana JO, Maldonado-Garza HJ, Zubía-Nevárez CI. Gruber-Frantz tumor: a rare pancreatic neoplasm. Rev Esp Enferm Dig. 2022;114(3):172-3.
- 18. Stefanova N, Kalinov T, Kolev N. Frantz Tumor: A case report of solid pseudopapillary tumor of pancreas. Cureus. 2023;15(7):e41698.
- 19. Qiu L, Trout AT, Ayyala RS, Szabo S, Nathan JD, Geller JI, et al. Pancreatic masses in children and young adults: Multimodality review with pathologic correlation. Radiographics. 2021;41(6):1766-84.
- Da M, Qian B, Mo X, Xu C, Wu H, Jiang B, et al. Inflammatory myofibroblastic tumors in children: A clinical retrospective study on 19 cases. Front Pediatr. 2021;9:543078.
- 21. Thompson LDR. Inflammatory myofibroblastic tumor. Ear Nose Throat J. 2019;100(5):520S-1S.
- 22. Da M, Qian B, Mo X, Xu C, Wu H, Jiang B, et al. Inflammatory myofibroblastic tumors in children: A clinical retrospective study on 19 cases. Front Pediatr. 2021;9:543078.
- Surabhi VR, Chua S, Patel RP, Takahashi N, Lalwani N, Prasad SR. Inflammatory myofibroblastic tumors: current update. Radiol Clin North Am. 2016;54(3):553-63.
- 24. Soyer T, Talim B, Karnak İ, Ekinci S, Andiran F, Çiftçi AÖ, et al. Surgical treatment of childhood inflammatory myofibroblastic tumors. Eur J Pediatr Surg. 2017;27(4):319-23.
- 25. Rebhandl W, Felberbauer FX, Puig S, Paya K, Hochschorner S, Barlan M, et al. Solid-pseudopapillary tumor of the pancreas (Frantz tumor) in children: report of four cases and review of the literature. J Surg Oncol. 2001;76(4):289-96.

Cite this article as: Hernández IB, de León Camargo DAP, Orozco LFZ, Irigoyen AE, Vega MDLV. Enhanced surgical planning with 3D modeling in pediatric surgical oncology: management of complex abdominal tumors in a low-income country. Int J Res Med Sci 2025;13:4903-12.